An experimental flow with zero skin friction throughout its region of pressure rise

By B. S. STRATFORD
National Gas Turbine Establishment, Farnborough

(Received 17 July 1958)

A flow has been produced having effectively zero skin friction throughout its region of pressure rise, which extended for a distance of 3 ft. No fundamental difficulty was encountered in establishing the flow and it had, moreover, a good margin of stability. The dynamic head in the zero skin friction boundary layer was found to be linear at the wall (i.e. $u \propto y^{\frac{1}{2}}$), as predicted theoretically in the previous paper (Stratford 1959).

The flow appears to achieve any specified pressure rise in the shortest possible distance and with probably the least possible dissipation of energy for a given initial boundary layer. Thus an aerofoil which could utilize it immediately after transition from laminar flow would be expected to have a very low drag. A design pressure distribution (besides having the usual safety margin against stall) should have a slightly more gradual start to the pressure rise than in the present experiment, as small errors close to the discontinuity can cause difficulty.

1. Introduction

In aerodynamics there is a commonly occurring need to decelerate, or diffuse, the flow of fluid relative to a surface. On an aerofoil, for example, diffusion is likely to be necessary on the rearward upper surface whether the aerofoil be isolated, as for an aircraft wing, or in cascade, as for turbo-machinery. Moreover, the diffusion is required in a fairly short distance and with a minimum loss of energy. § 6 of the previous paper (Stratford 1959) considered a flow having continuously zero skin friction throughout its region of pressure rise and this flow, as it will be shown, might be expected to achieve diffusion in the shortest possible distance with probably the lowest possible loss. After a preliminary theoretical discussion an experiment will be described testing the flow.

The pressure distribution for the present flow has been derived by specifying that the boundary layer shall be just at the condition of separation, without actually separating, at all positions in the pressure rise. Now at the condition of separation the local pressure gradient is the steepest which can be applied to the boundary layer, because an attempt to apply a steeper gradient would cause actual separation and breakdown of the flow. The present pressure distribution might be expected, therefore, to attain any given pressure rise in the shortest possible distance for a given initial boundary layer. This may be confirmed formally by a simple extension of the theory of the previous paper.

The second property of interest concerns the energy loss. Since the present flow is at all points at the condition of separation, the skin friction is continuously zero. Now 'zero skin friction' might at first suggest low loss, but in fact losses due to the pressure gradient tend to compensate for the reduction in skin friction. It is not immediately clear from the momentum equation whether the present flow provides a net gain over other flows as the pressure gradient term, $\delta^* dp/dx$, is not readily calculated. However, consideration of the rate of energy dissipation by the shear forces throughout the boundary layer indicates that for a given local mainstream velocity the dissipation per unit length of surface would vary only slightly with the shape of the boundary layer profile (the latter determines the skin friction). Thus, flow with zero skin friction would have about the same loss per unit length as other flows, but, because it has the shortest possible length, it would have the least possible final loss. This argument, based upon the energy equation for the boundary layer, is not exact, and so the result will be verified in the next paragraph using the theory of the previous paper.

The previous paper shows that for any boundary layer in a pressure rise the total head in the outer layer is equal to that at the corresponding point in the comparison layer ($C_p = 0$). In the sub-layer, on the other hand, the total head is higher than in the comparison layer, the difference almost certainly being greater the greater the pressure rise; at the wall, clearly, the difference is equal to C_p. The energy loss in a flow with pressure rise is therefore less than in one without; moreover, the energy loss is least, at a given value of x, in the flow which has the greatest pressure rise, i.e. the present flow, which is continuously at the separation condition. It follows that the energy loss at a specified pressure rise will also be least in the present flow.

The advantage of minimum energy dissipation may not of itself be particularly significant in practical applications. On an aerofoil, for example, if the pressure gradient were shortened and, say, the region of constant pressure lengthened in order to maintain the lift unchanged, then for a fixed transition point the drag may not be appreciably different. A worthwhile gain would seem likely, however, if advantage were taken of the shortness of the pressure rise to increase the proportion of the chord over which the pressure gradient were favourable, in this way delaying transition. Such an aerofoil might be expected to represent the most efficient type that is possible without artificial boundary layer control. Wortmann (1955, 1957), Eppler (1955) and Speidel (1955) have already carried out a considerable volume of work on a similar type of aerofoil, this being based on the concepts of Wortmann using the boundary layer theory of Truckenbrodt (1952), and Wortmann (1957) has obtained improvements of the order of 20 % over certain previous low drag sections. Wortmann's pressure distribution appears to be more gradual than in the present experiment, as will be discussed later in the paper.

2. Apparatus and methods

The apparatus, sketched in figure 1, consisted of an open return wind tunnel having an 8 in. square-working section, a 9/1 ratio contraction, and a nominally 2/1 two-dimensional diffuser leading via transition sections to a fan. The speed

in the working section was approximately 55 ft./sec. The test boundary layer was that growing on one side wall of the working section and diffuser, and in this region the top wall of the apparatus was transparent.

The design shape of the test wall is shown in figure 2. The pressure distribution specified for the design was estimated from the evidence on boundary layer separation available at the time; the design geometry was then obtained from

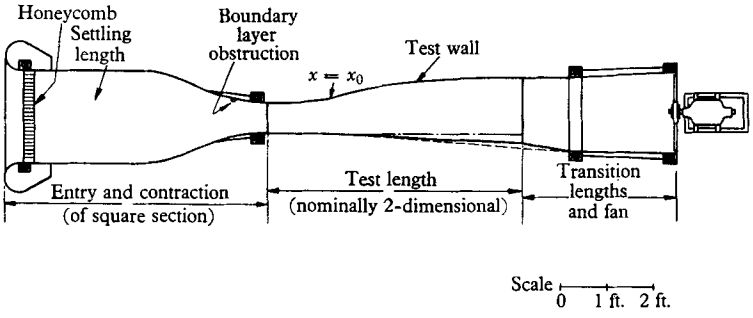

FIGURE 1. Plan-section sketch of the wind tunnel.

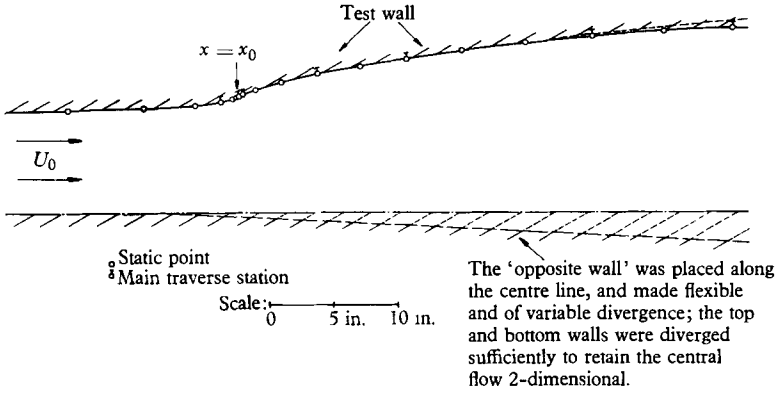

FIGURE 2. Design of the test section.

this pressure distribution by applying corrections, based on physical arguments, to the shape that would be predicted from one-dimensional inviscid flow theory. Since the design method was only approximate and the correct pressure distribution was known only roughly before testing, and since the boundary layer itself would affect the pressure distribution, provision was made for varying the divergence and shape of the opposite wall, in conjunction, if necessary, with building up the surface of the test wall.

One embarrassing feature of the design was that the aspect ratio of the test wall was very low. This feature resulted when the test wall was made long in order that the test boundary layer should be thick and its measurement thereby facilitated. Consequently, precautions were necessary in order to ensure that the flow within the test region was two-dimensional. Thus the top and bottom walls of the diffuser were diverged in order to compensate the displacement

thickness of their boundary layers; by this means the effective span of the flow, as checked by traversing for the displacement thickness of the top and bottom boundary layers, was held constant for the main tests to within about 1 %. The principal measurements were made at mid-span, on either side of which the flow was of uniform total head; the minimum width of uniform flow was about 40 % of the span, as shown by the traverses of figure 3.

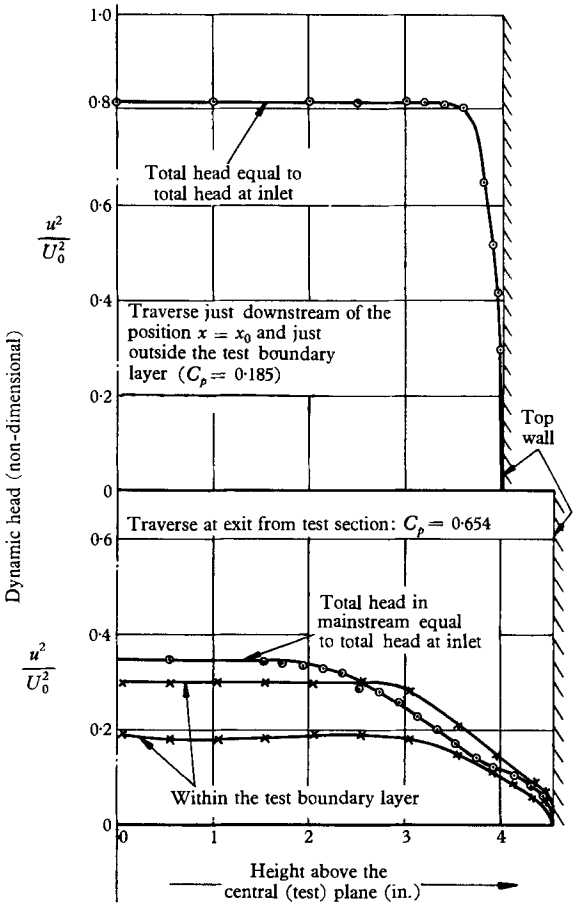

FIGURE 3. Spanwise variation of total head.

The method of finding the correct pressure distribution

The required flow was obtained by progressively earlier tripping of the test boundary layer in conjunction with the adjustments to the opposite flexible wall and slight building up of the test wall. In the final stages of this process the test boundary layer was thickened artificially just before entry to the working section. The correct and, at the time, unknown pressure distribution could thus be approached gradually even though the flow sought was everywhere close to separation.

The technique of artificial thickening was adopted when it was found desirable to shorten the original working section in order to reduce the thickness of the

boundary layers on the other walls. (Figure 1 is for the tunnel after shortening.) The artificial thickening resulted in an increase of 30 % in the value of the momentum thickness θ_0 at $x = x_0$. It was produced by a rectangular projection from the wall, this extending at first along the central 75 % of the span, but later along only the central 54 %. The projection had accurately ground surfaces in order to produce spanwise uniformity of loss, and it was preceded by a trip wire, this also being found necessary for obtaining spanwise uniformity. Traverses showed that despite the artificial thickening the test boundary layer had settled to a steady profile shape, to within about $2\frac{1}{2}$ % on velocity, well before reaching the region of pressure rise. Also its rate of growth $d\theta/dx$, and hence, presumably, its turbulence, was normal for a turbulent boundary layer without pressure gradient. The equivalent length x_0 of the test boundary layer in the main test was 35·2 in. giving a Reynolds number $x_0 U_0/\nu$ of $1{\cdot}0 \times 10^6$.

Simultaneously with the following through of the above process, small amounts of boundary layer control were applied to the other boundary layers, in particular at the corners, in order to prevent local separations or the development of large displacement thicknesses; these conditions could limit the pressure recovery attainable in the test section and even cause slight secondary flow on the test wall. Care was needed to prevent secondary flow near the control points themselves.

The process just outlined was straightforward in principle. In practice, however, it required much patient adjustment and modification. The greatest trouble that was encountered, apart from the embarrassments from the small aspect-ratio, occurred in correcting the pressure distribution near the discontinuity at $x = x_0$, the necessary correction itself being discontinuous at that point. A complicating factor was the sudden thickening of the test boundary layer on meeting the steep pressure gradient starting at the discontinuity.

The experimental pressure distribution obtained initially with a very thin boundary layer was quite close to design; the starting-point for the pressure rise was $\frac{1}{4}$ in. upstream of the design position, and the pressure coefficient at any given distance downstream of the starting-point was about 0·03 smaller than design. There was also a slight suction peak ($C_p = -0{\cdot}04$) just upstream of the discontinuity. The correct pressure distribution, i.e. that found necessary for giving continuously zero skin friction with the final thick boundary layer, had a pressure coefficient in most of the region of the pressure rise about 0·04 smaller than that of the initial experimental pressure distribution; this correct distribution was obtained as already described, the necessary distortions to the opposite wall being quite severe despite the smallness of the change required in C_p.

Observation techniques

Determination of the flow condition was based on the following techniques, the observations being considered in conjunction one with another.

(*a*) *Tuft behaviour.* Tufts indicated the steadiness and direction of the flow. The degree of unsteadiness became a good indication of the closeness to the separation condition.

(*b*) *Transition.* It being an open return tunnel, the chalk dust technique was used for indicating transition.

(*c*) *Static pressure distribution.* Readings from a multi-tube manometer indicated the smoothness of the distribution, its steadiness with time, and whether the maximum possible pressure rise was being obtained for a given initial boundary layer.

(*d*) *Substitution into the integrated momentum equation.* Ideally τ_0 could be obtained from the experiment by direct substitution into the momentum equation

$$\tau_0 = \frac{d}{dx}(\rho U_1^2 \theta) - \delta^* \frac{dp}{dx}. \tag{1}$$

However, the differentiation of the experimental values of $\rho U_1^2 \theta$ makes this method over-sensitive to error. A more satisfactory procedure is to integrate the momentum equation, thus obtaining

$$\left(\frac{\rho U_1^2 \theta}{\rho U_0^2 \theta_0}\right) = \left[1 + \int_{x_0}^{x} \frac{\delta^*}{2\theta_0} dC_p\right] + \frac{1}{\rho U_0^2 \theta_0} \int_{x_0}^{x} \tau_0 dx, \tag{2}$$

and to compare curves of the experimental values of

$$\frac{\rho U_1^2 \theta}{\rho U_0^2 \theta_0} \quad \text{and} \quad \left[1 + \int_{x_0}^{x} \frac{\delta^*}{2\theta_0} dC_p\right].$$

A difference between the curves indicates a non-zero skin friction force provided the flow is accurately two-dimensional.

(*e*) *Velocity traverses.* Standard theory for turbulent flow shows that there is a close relation between the skin friction and the height of the 'shoulder' which occurs very close to the wall in either the velocity profile or the dynamic head profile. Thus a qualitative estimate could be made of the closeness to separation just by looking at the Pitot traverse. The estimate could be made more precise by using the result of the previous paper that the skin friction is zero when, in effect, the shoulder in the dynamic head profile is zero or, more specifically, when the dynamic head close to the wall increases linearly from a zero value at the wall. However, since it was a part of the object of the experiment to verify this theory, agreement with it could be used only as additional corroboration.

The effect of turbulence on the Pitot reading

The Pitot readings have not been corrected for the effect of turbulence. Calculations for the main test suggest that the proportional effect on the local dynamic head could be appreciable, but that the effect on the momentum thickness should be small.

Variation of static pressure across the boundary layer

In positions very close to the discontinuity the wall is highly curved and the static pressure varies across the thickness of the boundary layer. Now the actual boundary layer at any station x would become the same as for an experiment which conformed to the conditions of the theoretical model (static pressure

constant across the thickness of the boundary layer at all positions) if both the static pressure at the station x were made constant and equal to that at the wall, and if it could be assumed that the difference upstream between the local and the wall static pressures did not affect significantly the total pressure in any streamtube at the station x. The latter would be reasonably true in the present experiment as the variation of static pressure across the boundary layer is found to be both small and confined to a short length of wall. Hence the present experimental results would correspond to those of an experiment conforming to the theoretical model if in the formula for θ,

$$\theta = \int_0^\infty (1-u/U)\,d\psi/U = \int_0^\infty (1-u/U)\,u\,dy/U, \tag{3}$$

the velocities were calculated from an equivalent dynamic head equal to the local total head minus the wall static pressure, the true volume flow, however, being retained in any streamtube. Consequently θ has been calculated on this basis.

3. Results

Characteristics of the flow

The flow had three important characteristics: (*a*) there was no fundamental difficulty in obtaining it, (*b*) it did appear to provide the shortest possible distance for a given pressure rise, and (*c*) it was stable.

(*a*) No fundamental difficulty was experienced in obtaining the flow with continuously zero skin friction; the relevant part of the test surface extended for just over 3 ft.

(*b*) The flow condition could be varied by altering the divergence and shape of the opposite wall. As far as could be ascertained, the condition for maximum pressure rise at any specified position on the test wall did coincide with the condition for continuously zero skin friction. For example, as the divergence of the diffuser was gradually increased the pressure rise at any given position on the test wall first increased to a maximum, which occurred when the skin friction had become effectively zero, it then remained almost constant for an appreciable range of divergence and, thereafter, it decreased. Attempts at improving upon the pressure rise given by the flow with continuously zero skin friction were never successful.

(*c*) The flow was found to be stable, and with the divergence just sufficient to reduce to zero the skin friction and to produce the maximum pressure rise, neither the losses, nor the steadiness of the pressure rise, were very sensitive to small changes in the passage divergence. In particular, a small increase in the divergence did not cause backflow. [Instead the displacement thickness of the test boundary layer increased sufficiently (up to a maximum of about 10 % of the total boundary layer thickness $\delta_{0\cdot99}$) to compensate the additional flow area, the skin friction remaining sensibly zero and the pressure distribution unaltered. This 'elasticity' in the boundary layer displacement thickness was made possible by the onset of a special regime of flow with a very high turbulence level close to the wall.]

The stability found for this flow is in contrast to the usual instability of turbulent flows near separation. In the present experiment the flow contained no dead-air region, while the boundary layers on the other three walls were controlled sufficiently to prevent separation; thus the geometry of the mainstream was virtually fixed. In most previous experiments, on the other hand, the mainstream geometry could vary either due to the presence of a dead-air region, or due to separation being imminent all round. Consequently, the usual instability found in previous experiments may be a result of the variable mainstream geometry rather than of the characteristics of the local boundary layer.

Quantitative results are shown in figure 4 onwards.

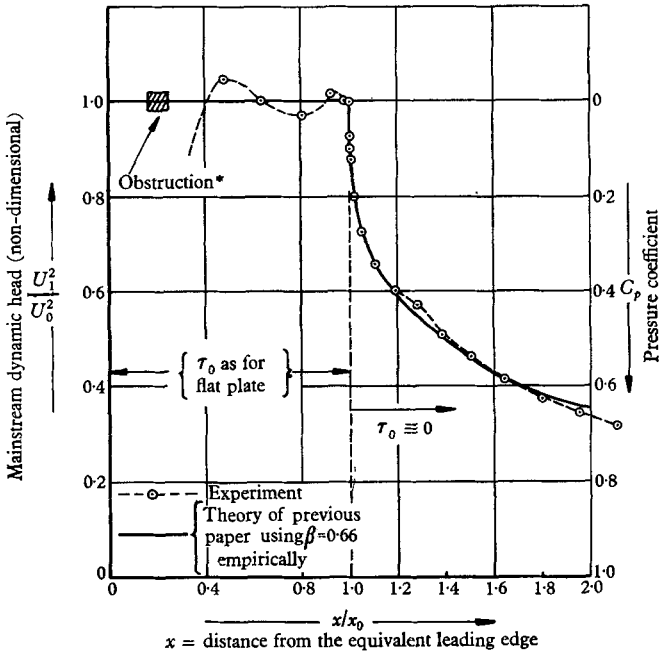

FIGURE 4. Pressure distribution for flow with zero skin friction ($R_0 = 10^6$). In the experiment the initial region (a length of about $\frac{1}{3}x_0$) was replaced by an equivalent obstruction, and the equivalence, including indirectly, the normality of the turbulence level, checked by boundary layer traverses.

4. Discussion of the results

The value of β

The immediate item of analytical data required from the experiment was the value of the factor 'β' necessary for completion of the theory. In figure 4 is shown a comparison of the experimental and 'theoretical' pressure distributions for producing continuously zero skin friction when a constant value of β, equal to 0·66, is used empirically in the theory; it will be seen that the fit of the curves is very good. (Most of the irregularities in the pressure distribution upstream of $x = x_0$ result from the distortions made in the opposite wall when setting the conditions in the main test length near and downstream of $x = x_0$.) The fact that β is of order unity supports the general concepts of the theoretical

method. It is notable how close an agreement is obtained using a value of β which is independent of x/x_0. The evidence is insufficient of course to show that there are not even small variations in β with x/x_0.

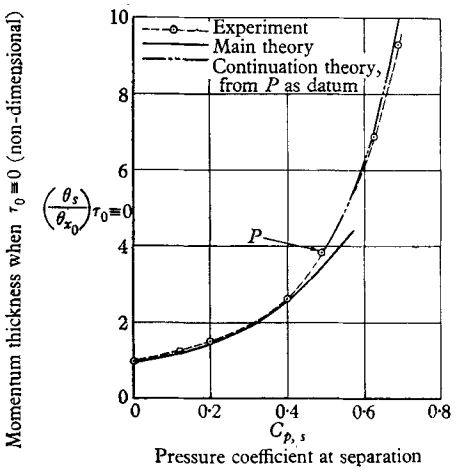

FIGURE 5. Momentum thickness of the boundary layer.

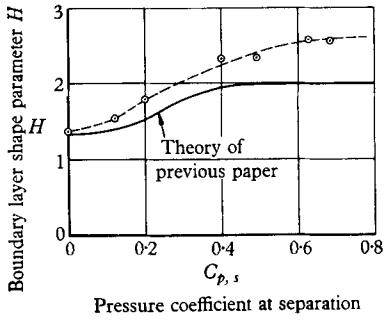

FIGURE 6. Values of the shape parameter $H = \delta^*/\theta$.

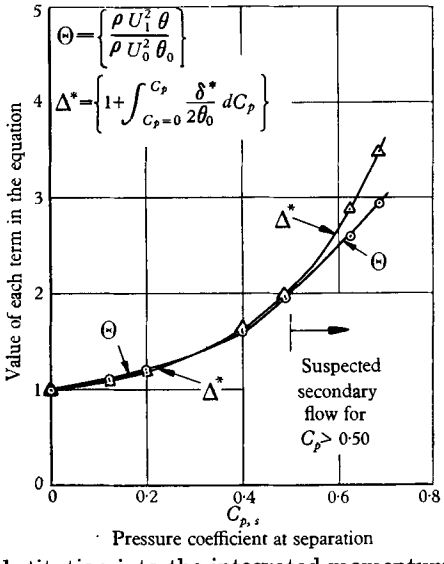

FIGURE 7. Substitution into the integrated momentum equation (2).

The main test

Some details from the main test, for which the pressure distribution was as in figure 4, are given in figures 5 to 8, together with the theoretical profiles for comparison in figure 9.

This main test provided the shortest pressure rise that it was found possible to achieve in the experiment, and it may be judged from the dynamic head profiles that the skin friction is zero, or very close to zero. The linear profile for the

dynamic head (figure 8), close to the wall in the inner layer, is visible particularly in the profiles for $C_p = 0{\cdot}122$, $C_p = 0{\cdot}200$ and $C_p = 0{\cdot}682$. The very slight shoulder in the profiles at $C_p = 0{\cdot}399$, $C_p = 0{\cdot}489$ and $C_p = 0{\cdot}624$, indicates an imperfection in setting the condition, so that the corresponding skin friction is still very slightly positive. (A special test to check that a linear profile is possible at these latter values for C_p was able to produce results such as curve '*b*' of figure 12.)

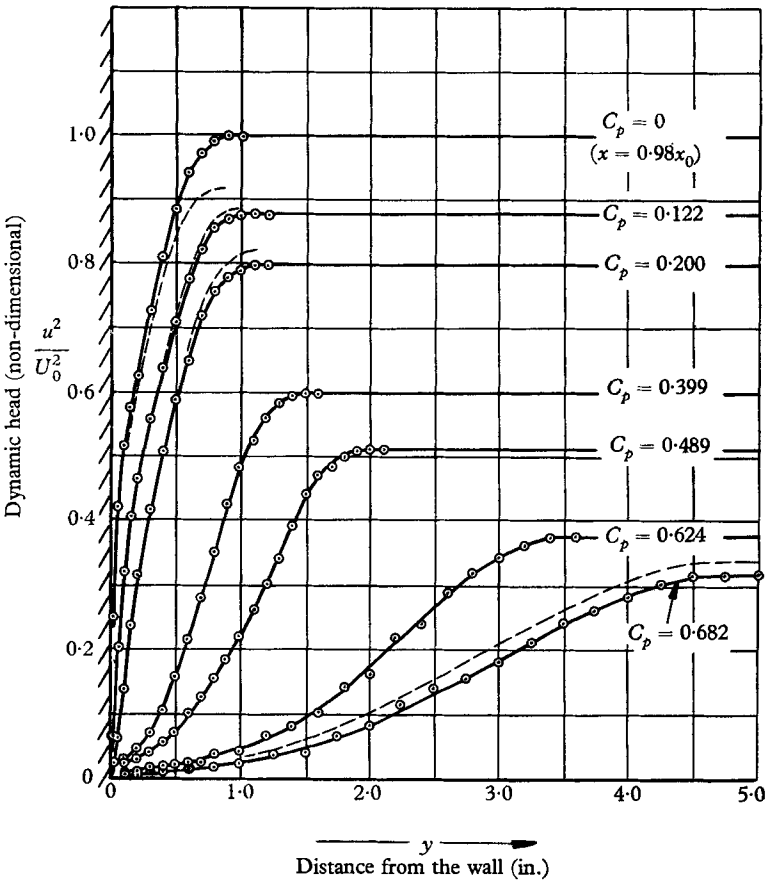

FIGURE 8. The dynamic head profiles. The full line profiles represent total pressure minus static pressure at the wall. Where the static pressure varies across the boundary layer the true dynamic head is represented by the broken lines. The C_p values refer to the wall.

At the condition of this test the tufts were beginning to become unsteady but there was no sign of backflow or serious oscillation. Examination of figure 7 shows that the flow is consistent with the integrated momentum equation with $\tau_0 \equiv 0$, up to $C_p = 0{\cdot}5$; above this value there is a discrepancy, the final momentum deficiency being about 15 % less than it apparently should be. Since the skin friction is certainly not negative it would seem that there was some loss of fluid from the later part of the test boundary layer, presumably by spanwise flow on that part of the test wall, despite the precautions taken; thus the results for this test are not accurate above, say, $C_p = 0{\cdot}5$.

When plotted against C_p, as in figure 5, the momentum thickness shows a very rapid increase above, say, $C_p = 0{\cdot}5$, at which position it has quadrupled its value at $x = x_0$. Comparison with figure 4 shows that the rate of increase with x would be greatest in the range just downstream of x_0. Figure 5 indicates reasonable agreement with the theoretical values for the momentum thickness. (If this is plotted as θ_s/θ_b against C_p, as in figure 5 of the previous paper, the theoretical values are independent of the empirical factor β. The agreement obtained, which is effectively the same as in the present figure 5, provides significant confirmation of the soundness of the theoretical concepts.)

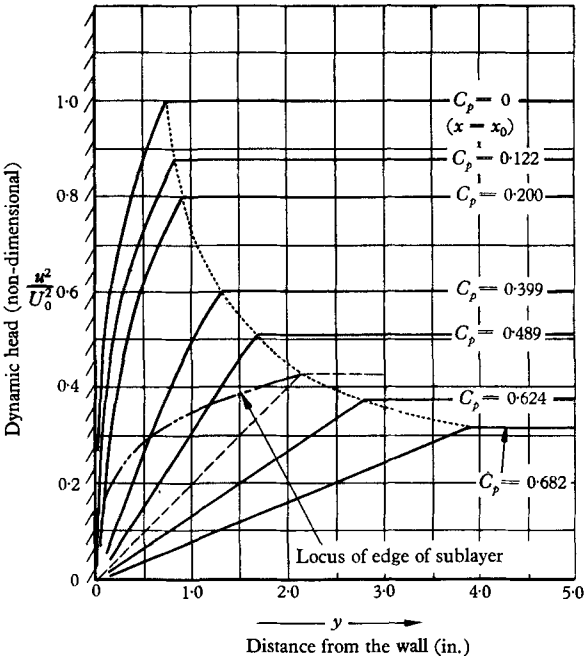

FIGURE 9. The theoretical dynamic head profiles calculated from the previous paper, for comparison.

The experiment confirms the linear dynamic head predicted theoretically for the inner layer near the wall. The experimental profiles, however, show a region of concavity. This is not surprising in view of the fact that the theoretical profiles have been idealized for simplicity of analysis. In terms of the theory the concavity is explained by a sharp fall-off in the value of the mixing length from the idealized linear value assumed for it. The conversion of a dynamic head profile with such a concavity to a velocity profile gives the hump characteristic of turbulent boundary layers near separation. (On the other hand, a hump is obtainable in the dynamic head profile itself as, for example, in the tests of figures 10 and 11, which will be discussed later.)

In using the results just quoted as confirmation of the theory the argument is not quite complete. Thus the theory suggests: first, that the skin friction falls to zero when the dynamic head becomes linear; and secondly, that the shortest possible pressure rise for a given initial boundary layer is obtained when the skin

friction is continuously zero. The experiment, on the other hand, verifies that the shortest possible pressure rise for a given initial boundary layer is obtained when the hump in the dynamic head profile close to the wall has been reduced to zero and the dynamic head has become linear, at all positions along the wall; it is only the almost circumstantial evidence provided by the behaviour of the tufts,

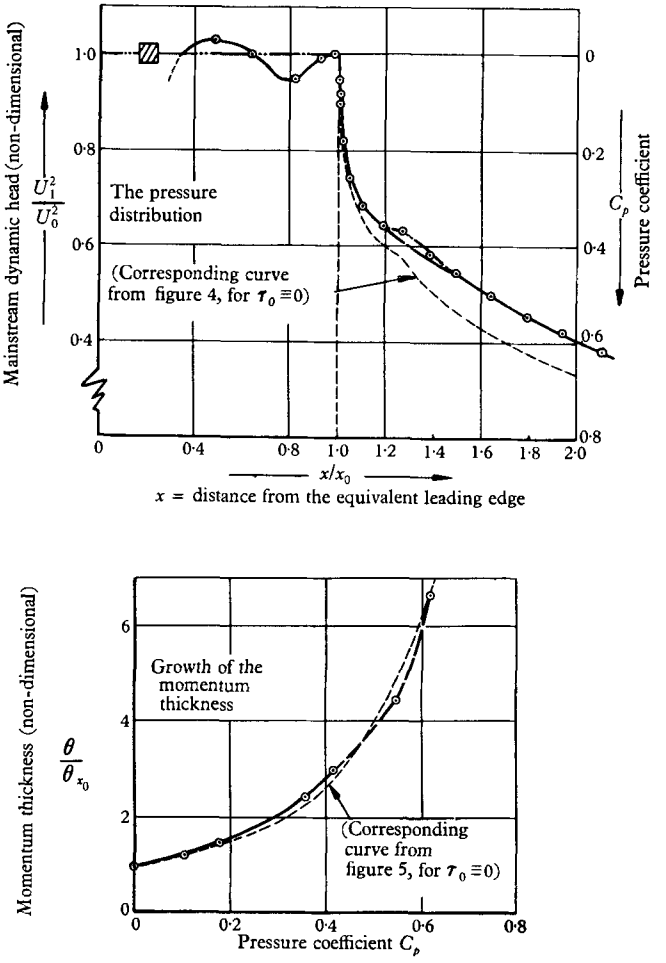

FIGURE 10. Details of the flow with a slightly slower pressure rise.

by substitution into the integrated momentum equation, by the steadiness of the pressure distribution, and by earlier qualitative ideas that the skin friction was related to the hump in the profile close to the wall, which confirms that this condition of a linear dynamic head coincides also with an effectively zero skin friction.

A slightly more gradual pressure rise

For comparison with the main test figures 10 and 11 show the effect of using a slightly more gradual pressure rise, the Reynolds number $x_0 U_0/\nu$ being maintained at the same value as before.

With the more gradual pressure rise the tufts indicated that the flow was very steady, the dynamic head profiles of figure 11 showing that it was appreciably away from separation. The effect of the skin friction on the increase of momentum deficiency was still small however, in comparison with the increase due to pressure gradient, as may be seen from the momentum equation in figure 11. It is not surprising, therefore, that the momentum thickness expressed as a

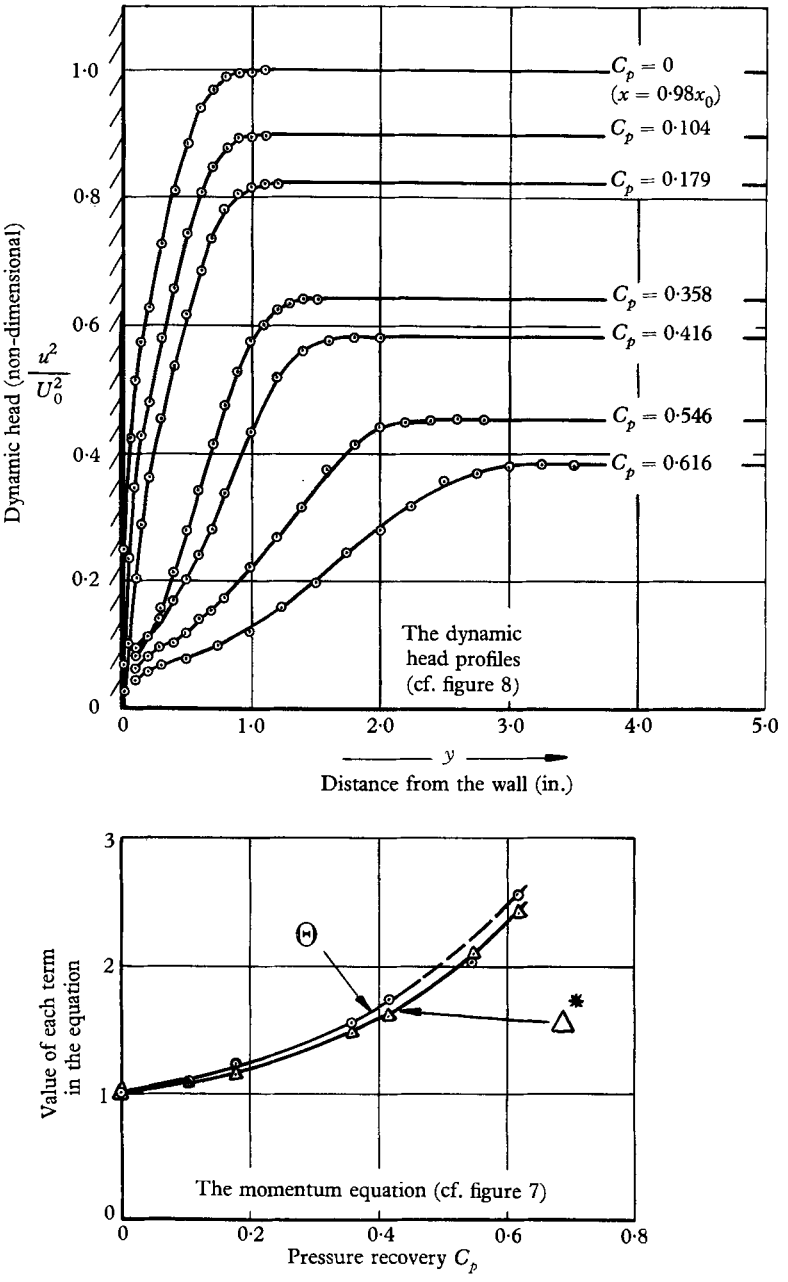

FIGURE 11. Further details of the flow with a slightly slower pressure rise.

function of pressure recovery, as in figure 10, was only a little greater than for the main test. (Considered from another viewpoint, θU_1^3 is related to the energy dissipation, which in turn may be related approximately to $\left[\int_0^x (U_1/U_0)^3\,dx\right]^{\frac{4}{5}}$. At, say, $C_p = 0{\cdot}5$, this last quantity had increased by only 8 % between the two tests.)

Although such a flow as represented in figures 10 and 11 would require a distance 50 % greater than for the flow with zero skin friction in order to achieve any specified pressure recovery, the pressure rise would still be very rapid, achieving, for example, a pressure recovery of $C_p = 0{\cdot}3$ in a length equal to 10 % of the length x_0, and $C_p = 0{\cdot}5$ in a length equal to two-thirds of x_0.

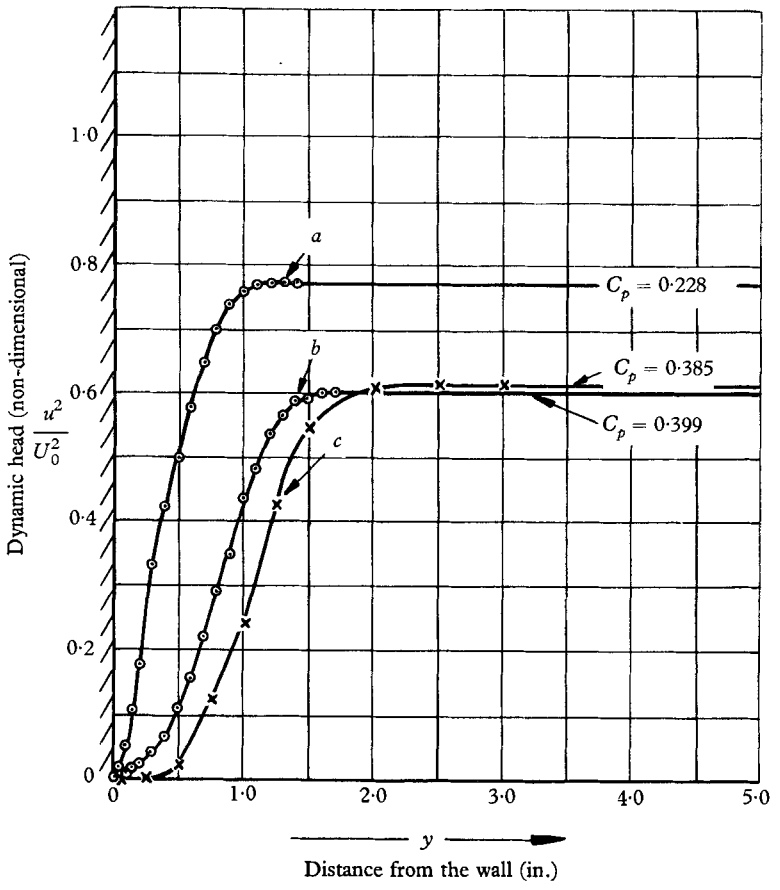

FIGURE 12. Some further dynamic head profiles.

Increased divergence—the regime with a very high turbulence level

Some further dynamic head profiles are shown in figure 12; these were all taken at different settings of the diffuser, profiles '*a*' and '*b*' each being for a slightly greater divergence rate than was used for the main test (figures 4 to 8).

Profile '*c*' of figure 12 is typical of the flow all along the test wall when the divergence was increased as much as was possible without producing a region

where the time-mean component of velocity was reversed. In this flow the tufts at the wall oscillated backwards and forwards violently indicating that the turbulence, if this name may be applied, was locally very intense. The static pressure as indicated by a sloping liquid manometer oscillated slightly; the maximum pressure recovery at each position was close to that for figures 4 to 8, while the minimum was approximately 7 % less, the time-mean being 0·01 or 0·02 less according to position. The flow as a whole, however, was still fairly steady. Since the pressure recovery at any specified position did not increase beyond that of the main test it follows that the increased divergence had been absorbed by an increase in the displacement thickness of the boundary layer. This is borne out by the shape of the profile; thus the dynamic head measurement was very close to zero for a depth of a $\frac{1}{4}$ in. from the wall, while the value of H, $= \delta^*/\theta$, had become 3·9, the largest measured in the experiment.

An increase in the divergence of the diffuser beyond that for profile 'c' of figure 12 produced a narrow region of backflow all along the test wall; the pressure rise became erratic, although the maximum value at any position still remained close to that for the main test. At a still greater divergence a complete breakdown of the flow occurred, with loss of pressure recovery and severe large scale fluctuations in the flow pattern and pressure distribution.

From a practical designer's viewpoint it is reassuring to know that, for the flow with effectively zero skin friction, the boundary layer, by means of its 'elastic' displacement thickness, allows some tolerance in the positioning of the wall. The tolerance is of the order of 10 % of the local boundary length thickness $\delta_{0\cdot99}$. For a diffuser, the tolerance would be available presumably on only a part of the periphery, as otherwise the flow might become unstable, due to having exceeded the divergence for maximum (time-mean) pressure recovery.

Mixing length distributions

Finally, figure 13 shows the distributions of mixing length calculated from some of the profiles. By using the equation for the inner layer profile obtained in the previous paper the values of the mixing length near the wall are readily shown to be given by

$$\left(\frac{\partial L}{\partial y}\right)_0 = \left\{\frac{2dC_p/dx}{[\partial(u^2/U_0^2)/\partial y]_0}\right\}^{\frac{1}{2}}, \tag{4}$$

where suffix 0 indicates values at $y = 0$. The values away from the wall have been obtained with the aid of a semi-theoretical estimate of the inertia forces in the inner layer.

These distributions of mixing length will not be very accurate as two differentiations of experimental profiles are necessary, together with the assumption that the skin friction is precisely zero; moreover, for an examination of the flow which obtains before the onset of the intense turbulence the dynamic head profile must be just linear, a critical condition which is not easily set in the experiment. Of the distributions shown in figure 13 those for curve 'b' of figure 12 and for '$C_p = 0{\cdot}200$' of figure 8 are close to this critical condition, for which the mixing length is seen to be not very different from that for the boundary layer on a flat plate. A more precise conclusion would not be justified by the evidence

available. For comparison Ludweig & Tillmann (1949) concluded for a turbulent boundary layer in a weak adverse pressure gradient that there was no change in the mixing length. On the other hand, for fully turbulent diffusers Squire (1950) and Stratford (1956) considered that the turbulence was greater than for the corresponding flow in a parallel pipe, Stratford (1956) suggesting that the increase

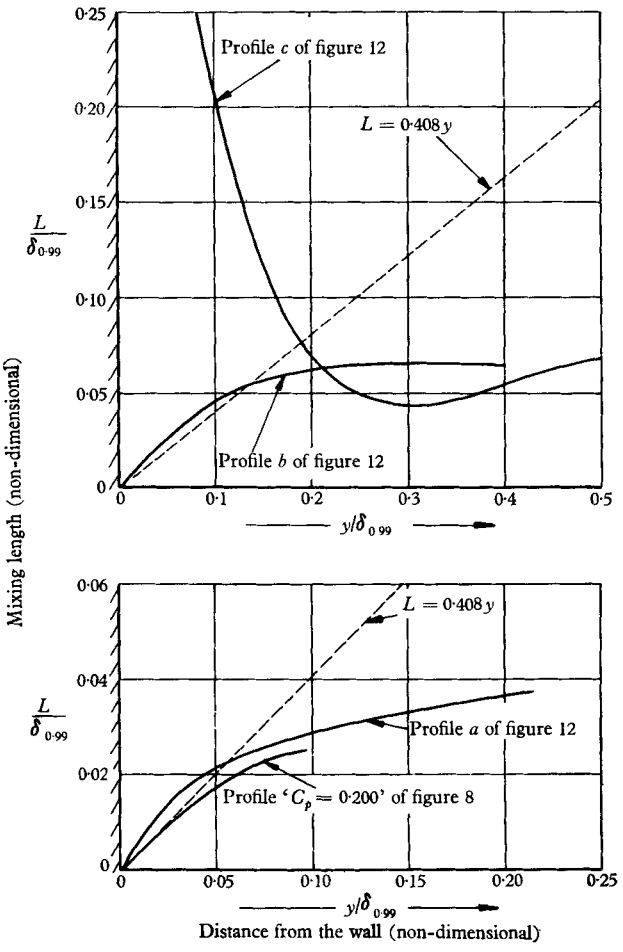

FIGURE 13. The turbulence level: some calculated mixing length distributions.

in the mixing length exceeded 30 %. It will be noticed that for none of the profiles in figure 13 is the value of $(\partial L/\partial y)_0$ less than 0·41, the value used for the flat plate boundary layer. The fact that β has been found to be less than unity in the present experiment is attributed to the rapid fall off in the mixing length away from the wall.

When the divergence is increased beyond that for the critical condition the turbulence as represented by $(\partial L/\partial y)_0$ at first increases, as for profile '*a*' of figures 12 and 13, and eventually becomes of a higher order of magnitude, as shown for profile '*c*', infinities nominally becoming involved. This type of behaviour supports the indication from the tufts.

Since the regime of intense turbulence does not cause an increase in the attainable pressure recovery at any position it does not affect the condition for separation; in particular it does not alter the theoretical prediction of the previous paper. There would, however, at a position of separation and flow reversal be a softening of the predicted discontinuity according to which $\partial u/\partial y$ at the wall changes from infinity positive to infinity negative.

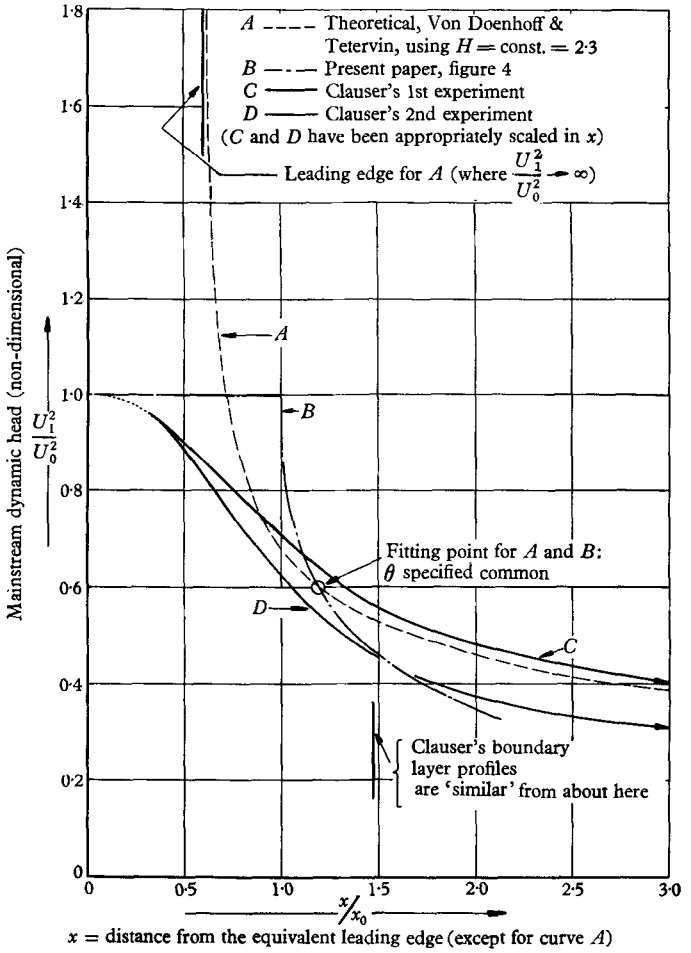

FIGURE 14. Comparison with other pressure distributions.

Comparison with other special pressure distributions

von Doenhoff & Tetervin (1943) have derived equations for a pressure distribution which would maintain the boundary layer at the separation condition, with similar velocity profiles, at all stations along the surface. In figure 14 this pressure distribution, calculated from their equations using the value $H = 2{\cdot}3$, is compared with the pressure distribution of the present paper. At the fitting point the values of H and θ are common to the two boundary layers, and so it might be expected that downstream of this point the pressure distributions should agree. In fact, they disagree.

Examination of von Doenhoff & Tetervin's analysis suggests that the derivation of this pressure distribution is not an appropriate application of their theory. Although the latter should be reasonably accurate for predicting separation when the profile shape is changing rapidly, there appears to be no evidence in support of their empirical auxiliary relations when a boundary layer near separation has a steady profile shape. In such a flow their relations become an extrapolation which, it would seem, could not be considered more than tentative.

In figure 14 are reproduced two experimental pressure distributions of Clauser (1954); each of these distributions gives a constant shape in the outer part of the boundary layer downstream of an initial settling length. For his first experiment Clauser considers that the bounday layer is far from separation while, for his second experiment, although this is closer to separation, he considers the skin friction still to be greater than zero. It would seem, therefore, that the pressure distribution of the present paper could be considered a reasonable extrapolation to zero skin friction from the two distributions of Clauser. The difference in the Reynolds number between Clauser's test and the present should cause only a very small effect. Comparison of velocity profiles using the variable adopted by Clauser, i.e. $(u-U_1)/u^*$, is not possible as $1/u^*$ $(=\sqrt{[\rho/\tau_0]})$ is infinite in the present test, where $\tau_0 = 0$.

Wortmann (1955, 1957) has produced pressure distributions for a constant form parameter H using the method of calculation of Truckenbrodt (1952). Although exact comparison is complicated by interpretation of the conditions at transition, Wortmann's experiments being for laminar flow aerofoils on which the close control of transition presented some difficulty, it would seem that the steepest pressure rise used by Wortmann is intermediate between Clauser's and that of the present experiment. Speidel's (1955) test of an aerofoil designed by Wortmann also appears to have a more gradual pressure rise than in the present experiment. Some of the difference in the rates of pressure recovery is probably due to the difference in Reynolds numbers.

The results of the present experiment check quite accurately both within themselves and with the predictions of the previous paper, and they are in at least qualitative agreement with Clauser's results and with the distributions of Wortmann. However, it would be desirable to have confirmatory evidence from a surface of larger aspect ratio before the accuracy of the present paper were regarded as established.

The value of n in the flat plate relationship, $u/U_0 = (y/\delta)^{1/n}$

Profiles were analysed for two positions upstream of the position $x = x_0$, figure 15 showing logarithmic and direct plots for a Reynolds number of $0{\cdot}64 \times 10^6$ $(= 10^{5{\cdot}8})$. It was concluded that the relation adopted in the previous paper, i.e. $n = \log_{10} R$, was reasonably satisfied near $R = 10^6$.

The experiment described in this paper was carried out in the Aeronautics Department of Imperial College, London. The author is indebted to the staff of that Department for stimulating criticism and advice, and to the Department of Industrial and Scientific Research for a grant which enabled the work to be undertaken.

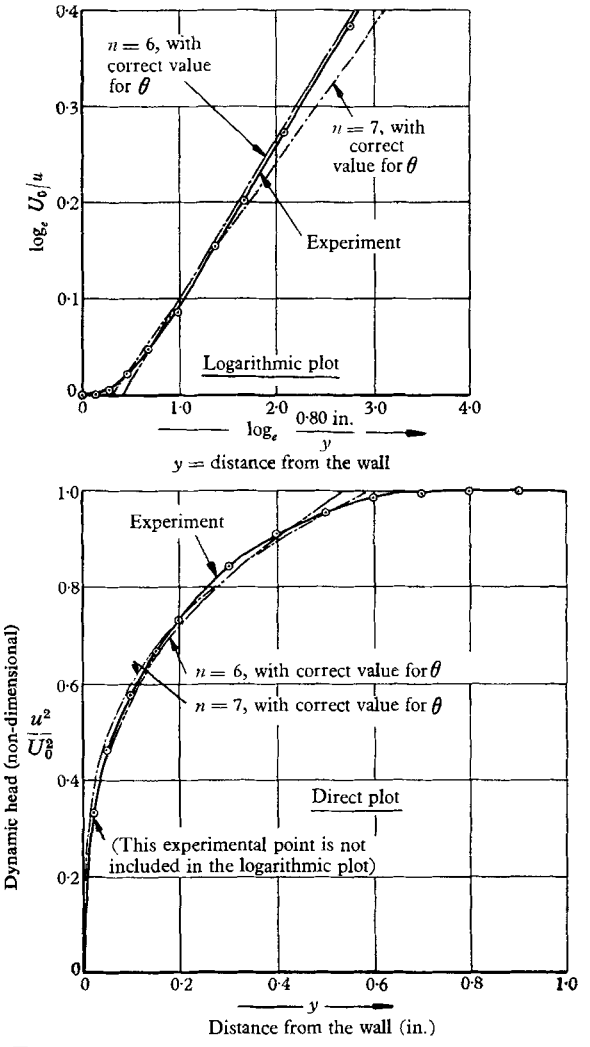

FIGURE 15. The value of 'n' when $R = 0{\cdot}64 \times 10^6$.

REFERENCES

CLAUSER, F. H. 1954 *J. Aero. Sci.* **21**, 91.

VON DOENHOFF, A. E. & TETERVIN, N. 1943 *Rep. Nat. Adv. Comm. Aero., Wash.*, no. 772.

EPPLER, R. 1955. *Z. Flugwiss.* **3**, 345 (British M.o.S. transl., in preparation).

LUDWEIG, H. & TILLMANN, W. 1949 *Tech. Mem. Nat. Adv. Comm. Aero., Wash.*, no. 1285 (transl.).

SPEIDEL, L. 1955 *Z. Flugwiss.* **3**, 353 (British M.o.S. transl., in preparation).

SQUIRE, H. B. 1950 *Rep. & Mem. Aero. Res. Coun., Lond.*, no. 2751.

STRATFORD, B. S. 1956 *Curr. Pap. Aero. Res. Coun., Lond.*, no. 307.

STRATFORD, B. S. 1959 *J. Fluid Mech.* **5**, 1.

TRUCKENBRODT, E. 1952 *Ingen.-Arch.* **20**, 211.

WORTMANN, F. X. 1955 *Z. Flugwiss.* **3**, 333 (British M.o.S. transl., in preparation).

WORTMANN, F. X. 1957 *Z. Flugwiss.* **5**, 228 (British M.o.S. transl., in preparation).